Journal of Marine Research, 56, 681–711, 1998

Influences of physical oceanographic processes on chlorophyll distributions in coastal and estuarine waters of the South Atlantic Bight

by P. G. Verity[1], J. O. Blanton[1], J. Amft[1], C. Barans[2], D. Knott[2], B. Stender[2] and E. Wenner[2]

ABSTRACT

Coastal and estuarine waters of the South Atlantic Bight are highly productive, with primary production of 600–700 gC/m^2/y. While controls and fate of this production are conceptually well understood, the importance of meteorology and physical circulation processes on phytoplankton has not received equivalent attention. Here, we describe the effects of wind stress and tidal currents on temporal and spatial distributions of phytoplankton biomass represented as chlorophyll *a* (chl *a*). Moored instruments were deployed and shipboard sampling was conducted in the North Edisto estuary (South Carolina) and adjacent inner shelf waters during four, two-week field studies in May and August 1993, and June and September 1994. Local wind regimes induced upwelling- and downwelling-favorable conditions which strengthened or reduced vertical density stratification in the coastal frontal zone, respectively, and shifted the location of the front. Chl *a* in shelf waters was more or less homogenous independent of the wind regime, while chl *a* on the estuary delta was generally vertically stratified. Within the estuary, chl *a* concentrations were positively correlated with the alongshore component of wind stress; chl *a* was not correlated with the weaker cross-shelf component of wind stress. Highest chl *a* occurred during strong downwelling-favorable events. The quick response time to wind forcing (6–12 hrs) implied a direct effect on chl *a* distributions and not a stimulation of growth processes. The source of the elevated chl *a* in response to wind forcing was apparently resuspension of settled and epibenthic algal cells. Tidal currents also influenced the vertical distribution and concentration of chl *a*. Time series sampling on the estuary delta showed that, with increasing velocity of ebb and flood tide currents, the relative contributions of pennate and centric diatoms with attached detritus and sand grains also increased, indicating that tidal resuspension of settled and epibenthic microalgae also occurred. Vertical stratification of chl *a* (highest concentrations near the bottom) began to degrade upon mixing by tidal currents with velocities as low as 10 cm/sec. Homogenization of 5–7 m water columns was fully achieved at velocities of 20–30 cm/sec. The data document the direct and comparatively immediate (timescales of minutes-hours) impact of tidal and wind energy on concentrations and distribution patterns of phytoplankton in coastal and estuarine waters of the South Atlantic Bight.

1. Skidaway Institute of Oceanography, 10 Ocean Science Circle, Savannah, Georgia, 31411, U.S.A.
2. South Carolina Wildlife and Marine Resources Department, P.O. Box 12559, 217 Ft. Johnson Road, Charleston, South Carolina, 29422-2559, U.S.A.

1. Introduction

Inner shelf waters of the South Atlantic Bight are very productive, averaging 600–700 gC/m^2/y (Thomas, 1966; Verity *et al.,* 1993). The source of this productivity is considered to be riverine input of new nutrients coupled with extensive remineralization within the water column and adjacent sediments (Yoder, 1985; Hanson *et al.,* 1988, 1990). Physical circulation processes regulate the availability and consumption of nutrients in these shallow waters. Specifically, a coastal salinity front is created and maintained by buoyancy input from freshwater discharge (Blanton and Atkinson, 1983; Blanton *et al.,* 1994b). This front inhibits the exchange of dissolved and suspended particulate materials with offshore waters (Blanton, 1981; Yoder, 1985), favoring recycling shoreward of the front. Seaward of the front, striking declines occur in concentrations of chlorophyll *a* (chl *a*), particulate organic carbon (POC), turbidity, and all major nutrients (Oertel and Dunstan, 1981; Yoder, 1985; Yoder *et al.,* 1993).

The balance between mixing and buoyancy forces determines circulation processes, and hence the productivity and fate of particles in inner shelf waters. Two major mechanisms, surface winds and tidal currents, regulate mixing. Wind stress at the air-sea interface imparts kinetic energy to the water column because momentum is transferred toward the seafloor where energy is ultimately dissipated. In shallow inner shelf waters, this momentum transfer reaches the sediment surface before most kinetic energy is lost, efficiently mixing the water column (Blanton, 1991). In addition, tidal currents on the U.S. east coast are strongest on the inner shelf at the Georgia/South Carolina border, where tidal motions account for 75–90% of the total energy of inner shelf waters throughout the year (Redfield, 1958; Pietrafesa *et al.,* 1985). Tidal amplitude is 2–3 m, tidal excursion is 5–8 km or more, and tidal mixing in shallow waters is sufficient to overcome the buoyancy resulting from heating and river discharge (Pomeroy *et al.,* 1993). The shallower the water column, the greater the mixing. It has been speculated that such strong vertical mixing may partially overcome attenuation of irradiance by high turbidity (Oertel and Dunstan, 1981), thus permitting the measured high rates of photosynthesis (Yoder and Bishop, 1985; Verity *et al.,* 1993). Calculations suggest that the vertical excursion time from surface to sediment for suspended particles in these waters ranges from only minutes to 1–2 hours (Verity *et al.,* 1993).

Despite this general understanding of the potential effects of mixing on primary productivity in inner shelf waters of the SAB, it is unknown whether or not mixing directly influences plankton and other particles there. The general conceptual model is that tidal energy regulates primary production in coastal environments (Cloern, 1991). This energy input has been proposed to result in a more efficient linkage between primary production and fish yield in these environments compared to nontidal waters (Nixon, 1988). However, empirical studies indicate that excessive tidal energy is associated with reduced phytoplankton biomass, perhaps due to light limitation of primary production (Monbet, 1992). Additionally, wind stress imparts mixing energy to the water column, but the effects are unknown. Do surface winds act to homogenize or concentrate suspended particles? Are chl *a* concentrations influenced by winds? Are the effects direct or indirect (e.g. stimulation of

productivity via nutrient injections: Yin *et al.,* 1996)? Is there a threshold of wind stress above which turbulent processes dominate biological processes (Therriault *et al.,* 1978)? Here, as part of a larger study of effects of circulation processes on transport of decapod larvae from shelf spawning/development sites into estuarine nursery grounds (Wenner *et al.,* 1998), relationships between surface winds, tidal currents, and temporal/spatial distributions of chl *a* are described.

2. Methods

The study site was the North Edisto estuary (32°34′ N, 80°12′ W) and adjacent coastal waters in South Carolina, U.S.A. (Fig. 1). It is a relatively short estuary with simple bathymetry; it is surrounded by *Spartina*-dominated salt marshes; and it has only local freshwater inflow with minimal vertical stratification (Nummedal *et al.,* 1977; Matthews and Shealy, 1978). The estuary exits to the ocean through a narrow, deep (20 m) inlet, and over a relatively shallow ebb-tidal delta which protrudes seaward of the inlet throat. Four study periods each of two weeks duration were completed in May and August 1993, and June and September 1994. These periods were chosen for two principal reasons: they included periods when upwelling- and downwelling-favorable winds, respectively, are more likely to occur, and they coincided with predicted periods of ingress into the estuary by pelagic postlarvae of white shrimp and blue crab (Blanton *et al.,* 1994a, 1997).

A combination of moored instrumentation and shipboard samples was utilized for temporal and spatial resolution of currents, water masses, meteorology, and phytoplankton biomass (chlorophyll *a*). One mooring (M2 in Fig. 1) was positioned on the inner shelf to assess the response of alongshore and cross-shelf currents to wind forcing, while another (M1) was deployed within the deep (20 m) inlet channel to record currents, subsurface pressure and density. Deep channels into estuaries provide the principal conduit for shelf water into estuaries (Garvine, 1991). Data from M1 documented subtidal flow through the inlet in response to inner shelf events but was not intended to provide detailed current structure across the estuary; e.g., Kjerfve and Proehl (1979). Instruments on both moorings (see below) were placed in the lower half of the water column.

a. Moored instruments

Mooring M1 was placed on a relatively flat ledge to the side of the main channel (to avoid ship traffic) in 15–18 m, depending on season/year (the main channel is 21 m deep). Mooring M2 was located 18 km offshore at the 14 m isobath. Both were in place typically for about four weeks during each study period, except that M1 was not deployed during June 1994 and M2 was not deployed in September 1994. Two InterOcean Systems, Inc. S4 current meters and two Sea-Bird Electronics, Inc. SEACAT data loggers were deployed at each site to measure currents, temperature, and conductivity at two levels in the vertical and subsurface pressure at the bottom. Salinity and density (σ_t) were derived from conductivity, temperature, and pressure. The sampling rate for all instruments was six minutes (0.1 hour).

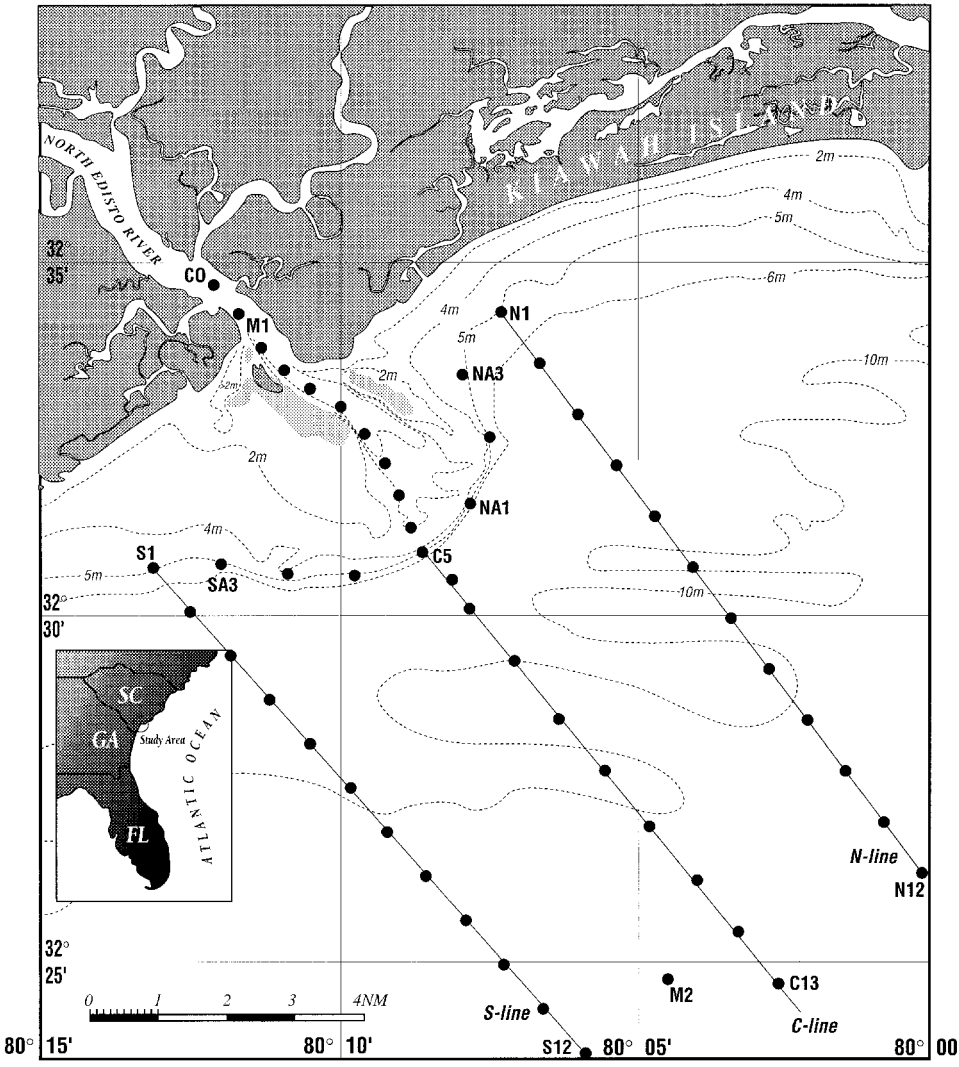

Figure 1. North Edisto estuary, delta, and inner shelf study region. Current meter mooring locations were at stations M1, M2, NA3, NA1, and SA3.

Wind speed and direction, barometric pressure, and air temperature were monitored hourly at Folly Beach (FBIS1), a nearby C-MAN (Coastal-Marine Automated Network) station which is maintained by NOAA (National Oceanic and Atmospheric Administration). FBIS1 is about 30 km E-NE of the study site and represents local conditions. Wind speed and direction files were converted to *x*- and *y*-components. Corresponding surface wind stress components were calculated by an iterative technique which adjusted wind speed to a 10 m level and used a variable drag coefficient proportional to magnitude of wind speed (Blanton *et al.,* 1989a).

b. Shipboard sampling

Additional information on temporal and spatial scales of currents, water masses, and chl *a* were provided by hydrographic sampling aboard the R/V *Anita* and R/V *Blue Fin.* The R/V *Blue Fin* generally conducted daily offshore surveys to map the structure of the coastal frontal zone and associated chl *a* distributions. For the August 1993 experiment, these inner shelf transects alternated along the N-line and S-line of stations perpendicular to shore and then parallel to the ebb tide delta (Fig. 1), to determine potential systematic differences north or south of the estuary delta. A transect approximating the N-line was sampled in May 1993, and in 1994 the N- and S-lines were collapsed into one central line. Sampling was primarily restricted to nighttime flood tides because of the related interest in ingress of shrimp and crab postlarvae (Wenner *et al.,* 1998). The timing of these offshore surveys was set to reach the ebb tide delta at maximum flood. Concurrently, the R/V *Anita* was stationed in the estuary throat adjacent to mooring M1, and sequentially sampled three positions laterally across the throat as quickly as possible, throughout nighttime flood tides. Data from the three throat locations have been combined in the present report.

Each vessel was equipped with identically configured Sea-Bird Electronics SBE-25 Sealogger CTDs, and identical data logging, calibration, and post-cruise analyses were used (Blanton *et al.,* 1994a, 1997). CTDs sampled at 4 Hz and downcast data were depth-averaged into 1.0 m bins. Salinity and density were calculated from the conductivity, temperature, and depth profiles using standard algorithms. Both CTDs were interfaced with SeaTech fluorometers configured for chl *a* fluorescence. They were calibrated at the same time on the same phytoplankton cultures before each cruise, and also calibrated during each cruise using natural plankton samples, extracted in acetone in the dark and measured using a Turner Designs fluorometer (Blanton *et al.,* 1994a, 1997).

c. Intensive sampling

Two special time series studies were conducted in June and September 1994. S4 current meters were deployed 1 m above bottom at two (June 1994: SA3, NA3) or three locations (September 1994: SA3, NA1, NA3) along the arcuate delta surrounding the estuary mouth (Fig. 1). Current velocity was recorded at 3-minute intervals. CTD and fluorescence profiles were conducted aboard ships adjacent to the current meters at intervals of 45–60 minutes. Niskin bottle samples from surface and bottom waters were prepared for brightfield and epifluorescence microscopy according to Verity and Sieracki (1993). Planned duration of sampling was 25 hours because the tidal cycle was 12.48 hours.

3. Results

a. General patterns

The alongshore component of wind stress is the principal forcing for coastal currents and wind-driven sea level fluctuations. When wind stress is upwelling-favorable (local wind from the SW), surface waters are advected offshore and replaced by deeper water brought in from offshore (Fig. 2). The coastal front is spread seaward and the strength of vertical

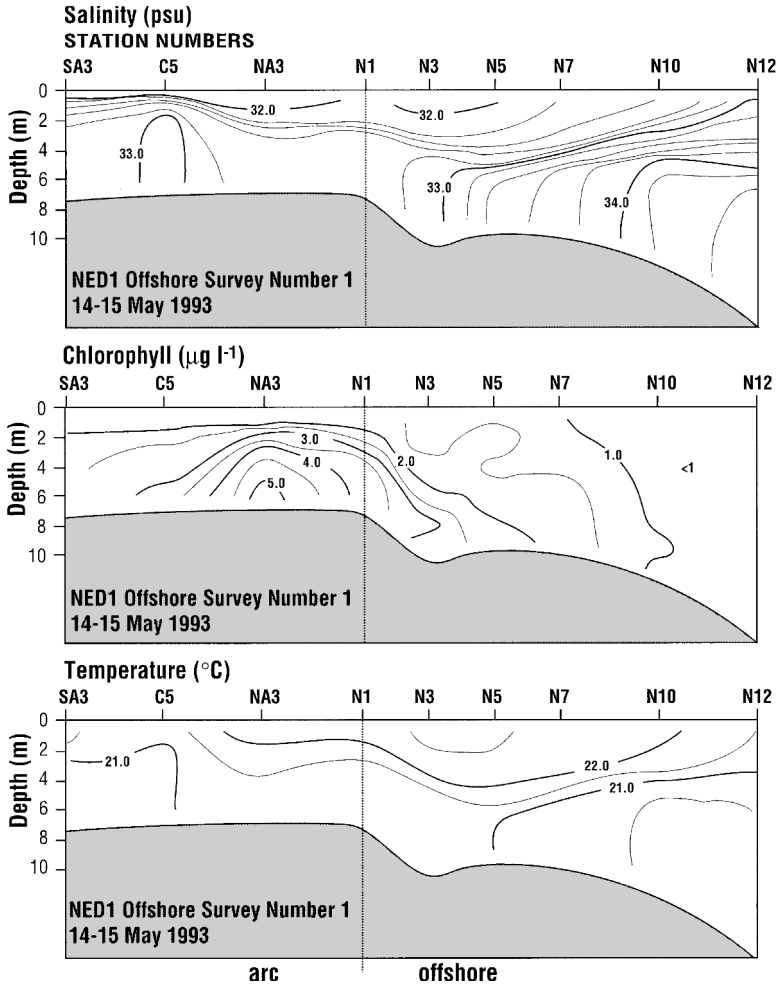

Figure 2. Typical profiles of salinity, chlorophyll *a,* and temperature across the inner shelf off the North Edisto estuary, under upwelling-favorable wind regime.

stratification increases. Note in Figure 2 that stations N1 to N12 are perpendicular to shore, while stations NA3 to SA3 are along the tidal delta ca. parallel to shore (the dotted vertical line in Figure 2 represents the change in orientation of the cruise track). The shelf transects began at the outer most station at slack low tide and reached the delta by mid-flood (2–3 hrs later). Thus, the nose of the front near N3 advected shoreward with the flooding tide and reached the delta by the time the ship arrived. In contrast, when winds are downwelling-favorable (local wind from the NE), near-surface waters are advected shoreward, near-bottom waters are carried seaward, the front is strengthened close to shore, and vertical stratification is diminished (Fig. 3). Downwelling circulation provides the most efficient vertical mixing. Vertically stratified water which typically appeared on the mid-outer portion of the transect during upwelling-favorable winds was instead vertically mixed.

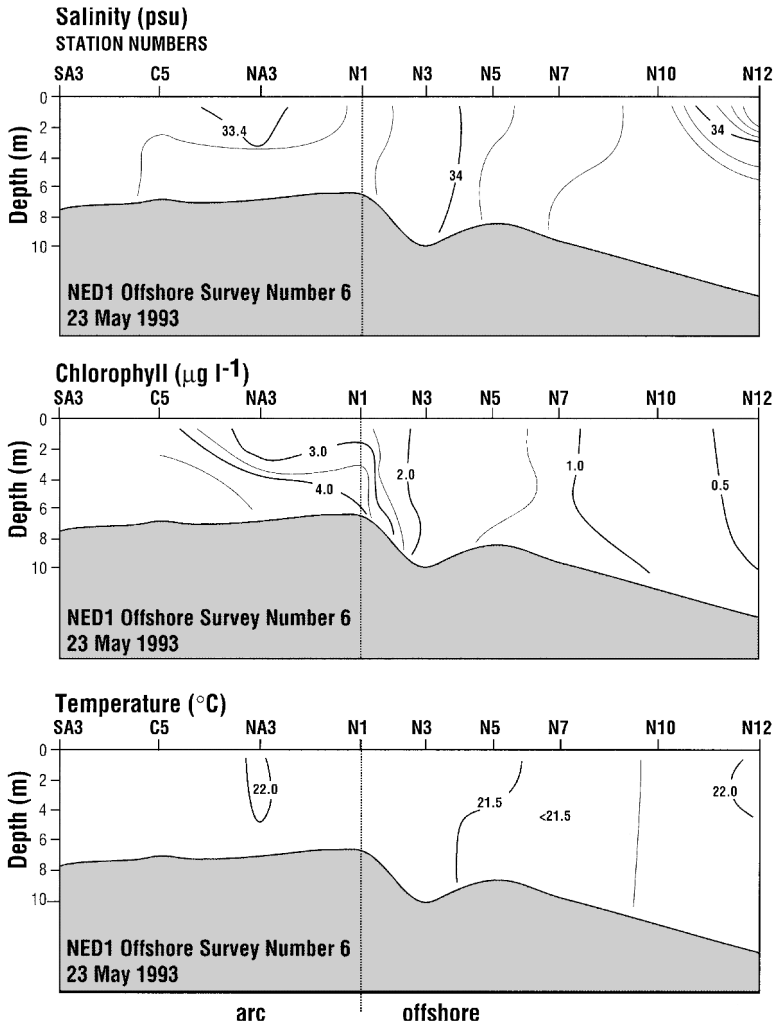

Figure 3. Typical profiles of salinity, chlorophyll *a,* and temperature across the inner shelf off the North Edisto estuary, under downwelling-favorable wind regime.

The vertical distributions of chl *a* and hydrographic parameters differed (Figs. 2–3). In inner shelf waters, chl *a* was typically homogenous independent of the effects of upwelling- or downwelling-favorable winds on salinity/temperature distributions. In contrast, chl *a* on the delta was typically stratified independent of winds, except that well-mixed plumes of chl *a* occurred down-wind (toward the estuary mouth on flood tides) during strong downwelling-favorable winds (Fig. 3). Mean water column concentrations of chl *a* decreased asymptotically with distance offshore from the estuary delta (Fig. 4). The data in Figure 4 represent eight transects across the inner shelf in May 1993, but similar functional relationships, albeit with slightly different slopes, were observed in other

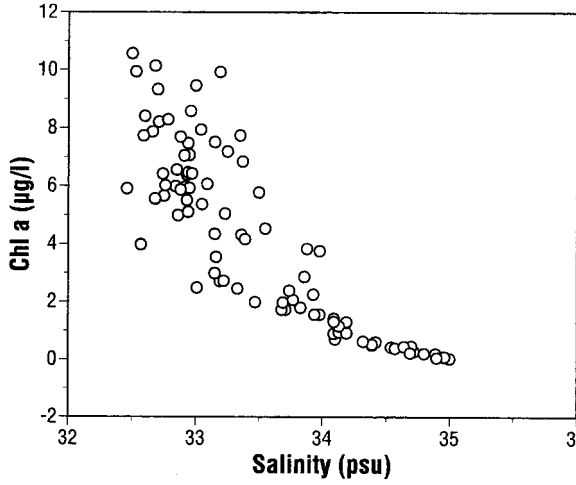

Figure 4. Relationship between chlorophyll *a* and salinity during transects across the inner shelf in May 1993. Data points represent mean water column chl *a* concentrations and salinities calculated from CTD profiles binned at 1 m intervals.

seasons and years. These data imply that the estuary and/or delta was a significant source of chl *a* for inner shelf waters.

Details of the vertical distributions of chl *a* from a typical transect are illustrated in Figure 5, which depicts chl *a* at any given depth in a vertical profile as a fraction of chl *a* at the bottom, versus the depth of that sample as a fraction of bottom depth. In open shelf waters (Fig. 5a), the following characteristics apply: (a) rarely does chl *a* at any depth exceed that at the bottom; (b) rarely is chl *a* at any depth $<$30–40% that at the bottom; and (c) the majority of depths contain chl *a* similar to that at the bottom (mean ratio = 0.80, SD = 0.19, n = 853). This pattern describes a fairly homogenous distribution of phytoplankton biomass on the inner shelf. In contrast, the following characteristics describe pigment distributions on the estuary delta (Fig. 5b): (a) rarely does chl *a* at any depth exceed that at the bottom; (b) near-bottom samples do not have low chl *a* compared to other depths; and (c) near-surface samples can have either high or low chl *a* compared to bottom samples. This pattern indicates estuarine waters with near-bottom pigment maxima which are occasionally redistributed through the water column.

b. Effects of winds

The preceding data illustrate general patterns in the horizontal and vertical distributions of chl *a* in estuary and shelf waters. These patterns, however, were dynamic. In the estuary throat, the highest chl *a* concentrations during a tidal cycle invariably occurred at intermediate salinities, albeit with seasonally different salinity scales (compressed in spring, broadened in autumn). To interpret this pattern, all CTD profiles in the estuary throat over four sampling seasons were combined into one dataset, which was then

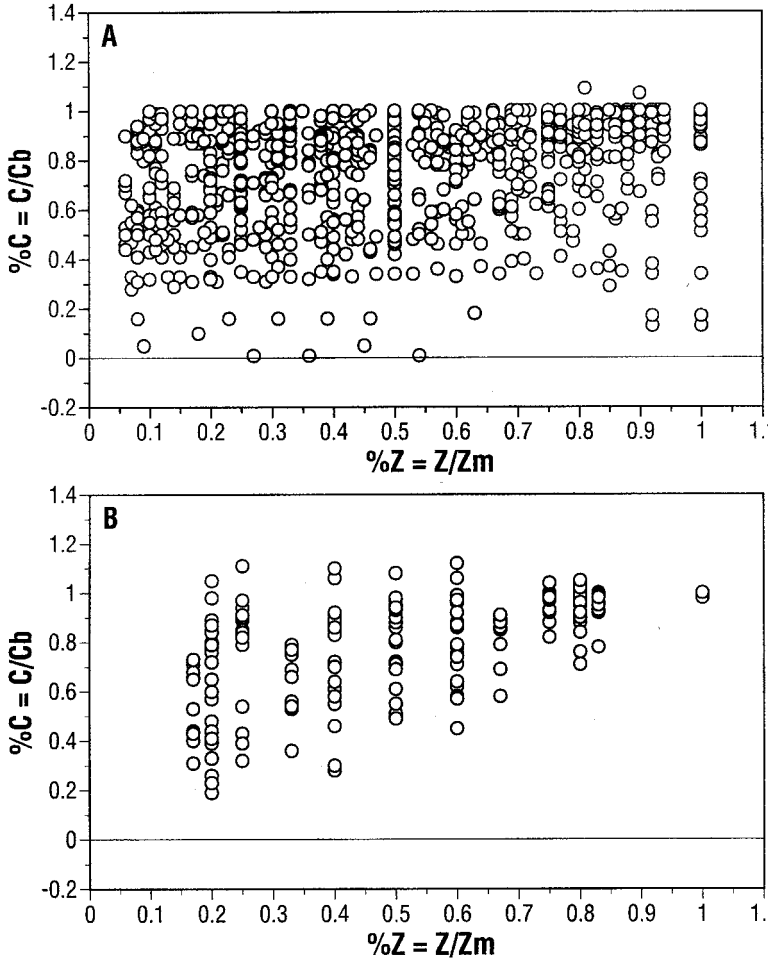

Figure 5. Relationships between the concentration of chl *a* at any given depth as a fraction of chl *a* in bottom samples, and the depth of that sample as a fraction of the bottom depth. Data from vertical profiles in (a) inner shelf waters, and (b) estuary throat.

segregated according to wind direction and velocity (Figs. 6–7). Strong (>7.5 m/sec) upwelling-favorable winds were associated with a narrow range of chl *a* concentrations occurring within a narrow range of high salinity waters (range = 1–2 PSU) (Fig. 6a). In contrast, strong downwelling-favorable winds were associated with a broad range of chl *a* occurring within a broad range of salinities (range = 6 PSU) (Fig. 6b). Note that the highest chl *a* concentrations occurred at higher salinities and these samples were collected during flood tides: strong downwelling-favorable winds somehow induced increases in chl *a* as the tide flooded into the estuary.

Weak upwelling-favorable winds were associated with a range of chl *a* similar to that

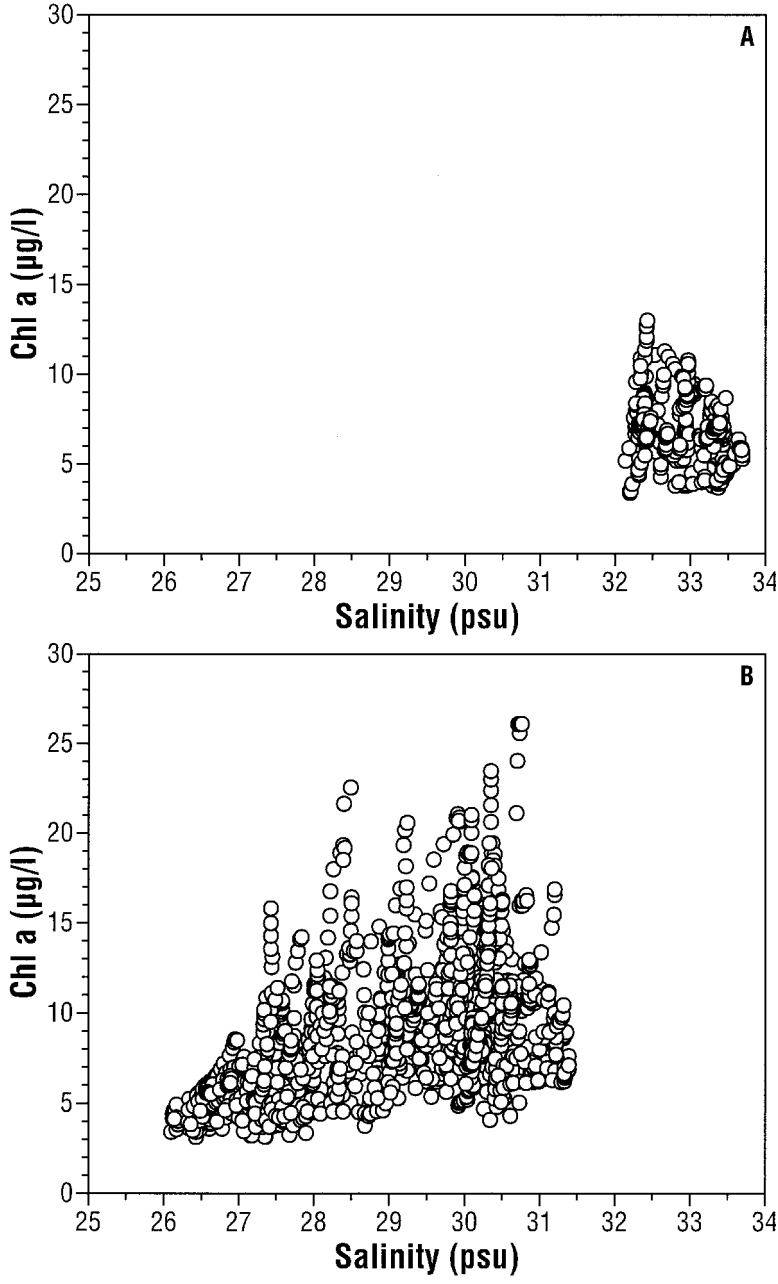

Figure 6. Relationships between chl *a* and wind velocity in CTD profiles collected during flood tides in the estuary throat. All data from 1994 were combined and partitioned according to wind direction and speed. (a) Strong upwelling-favorable conditions (local winds from SW with velocities >7.5 m/sec). (b) Strong downwelling-favorable conditions (local winds from NE with velocities >7.5 m/sec).

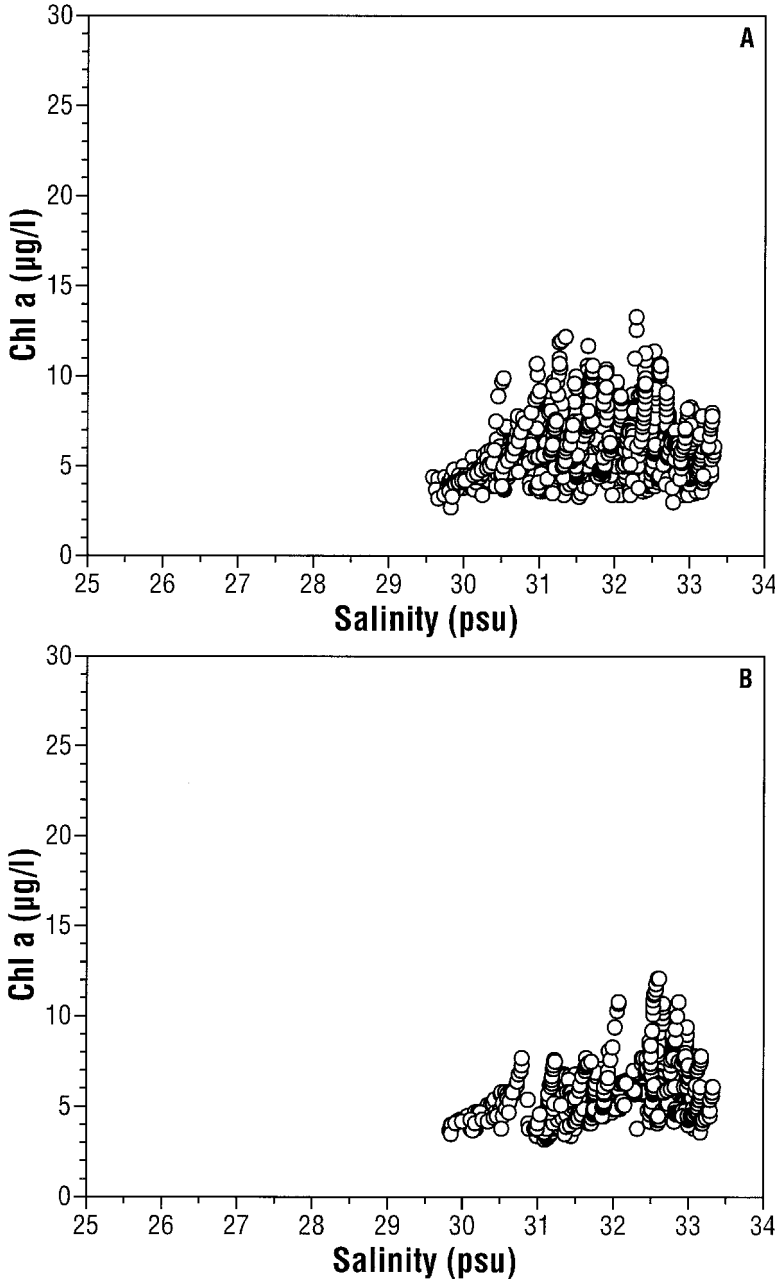

Figure 7. Relationships between chl *a* and wind velocity in CTD profiles collected during flood tides in the estuary throat. All data from 1994 were combined and partitioned according to wind direction and speed. (a) Weak upwelling-favorable conditions (local winds from SW with velocities <7.5 m/sec). (b) Weak downwelling-favorable conditions (local winds from NE with velocities <7.5 m/sec).

observed under strong upwelling, but with a broader salinity range (3–4 PSU) (Fig. 7a). Weak downwelling-favorable winds were associated with a range in chl *a* similar to that for weak upwelling, with a similar salinity range (3–4 PSU) (Fig. 7b). Thus the apparent relationship between chl *a* and salinity was primarily determined by increases in chl *a* during strong downwelling events.

Various temporal patterns in hydrography and chl *a* in the estuary throat were apparent in each season: an example is illustrated from May 1993 (Fig. 8). Water temperature increased during May 13–19, decreased during May 19–23, and increased again through May 27, while salinity generally increased the entire time. Neither showed much vertical structure, and sigma-*t* indicated considerable mixing. Chl *a* showed a temporal trend in concentration similar to that in salt content, but with clear vertical stratification and highest concentrations near-bottom (Fig. 8). (The fluorometer sensitivity range was set too low for this first field season, so near-bottom chl *a* values of 5.6 µg/l on May 24–25 were minimum estimates; this was corrected on the three subsequent field seasons).

The explanation for the temporal pattern in Figure 8 was apparently the effect of wind on water mass distribution and on intensity of vertical mixing. Wind stress was filtered with a 3-hr lowpass filter (3 hlp) to remove high frequency noise, and the wind stress vectors were rotated 50 degrees counter-clockwise, so that the principal axis paralleled the local shoreline. Figure 9 illustrates the *y* (alongshore) component of 3 hlp wind stress compared to mean chl *a* concentrations in the estuary throat, for the September 1994 field seasons (other seasons not shown for editorial brevity). In each season, the temporal pattern in chl *a* concentration was similar to that in alongshore winds: increased wind stress coincided with increased chl *a,* and calm periods co-occurred with little change in chl *a.* Comparatively weak winds occurred during sampling in 1993, while June and September 1994 exhibited stronger upwelling- and downwelling-favorable events, respectively. Comparison of the different wind regimes in June and September 1994 indicated that the direction of alongshore wind stress was not as important as the intensity in influencing chl *a* concentrations. In June 1993, both ships sampled different locations in the estuary throat and observed similar patterns between wind and chl *a,* albeit with differing chl *a* concentrations.

Data on winds and chl *a* from the four field seasons were combined and compared (Figs. 10–12). Wind speed and wind stress values were averaged for each ca. 4–6 hour sample period plus the preceding 6 hours, because 6–12 hours are required for the circulation field to respond to wind reversals (Blanton *et al.,* 1989b). These wind data were compared to mean water column chl *a* averaged during the 4–6 hour sample periods in the estuary throat. When the mean wind speed included all directional components, a significant linear relationship ($P < 0.01$) with chl *a* was observed (Fig. 10), and the correlation coefficient indicated that mean wind velocity explained 32% of chl *a* variance. When chl *a* was regressed against the *alongshore* component of the wind speed (Fig. 11a), the correlation coefficient increased to 40% ($P < 0.001$). Chl *a* was also significantly ($P < 0.001$) correlated with the maximum alongshore wind speed observed during each

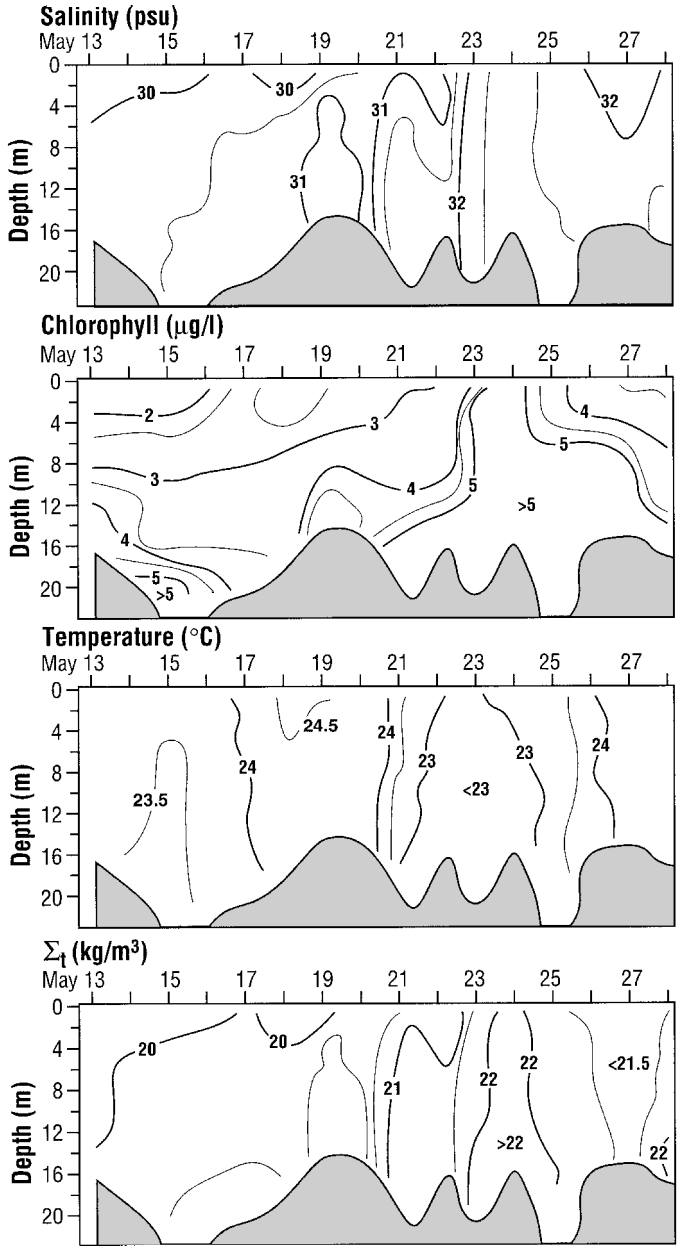

Figure 8. Time versus depth plots of salinity, chlorophyll *a,* temperature, and sigma-*t* during the period of maximum flood tidal currents in the estuary throat in May 1993.

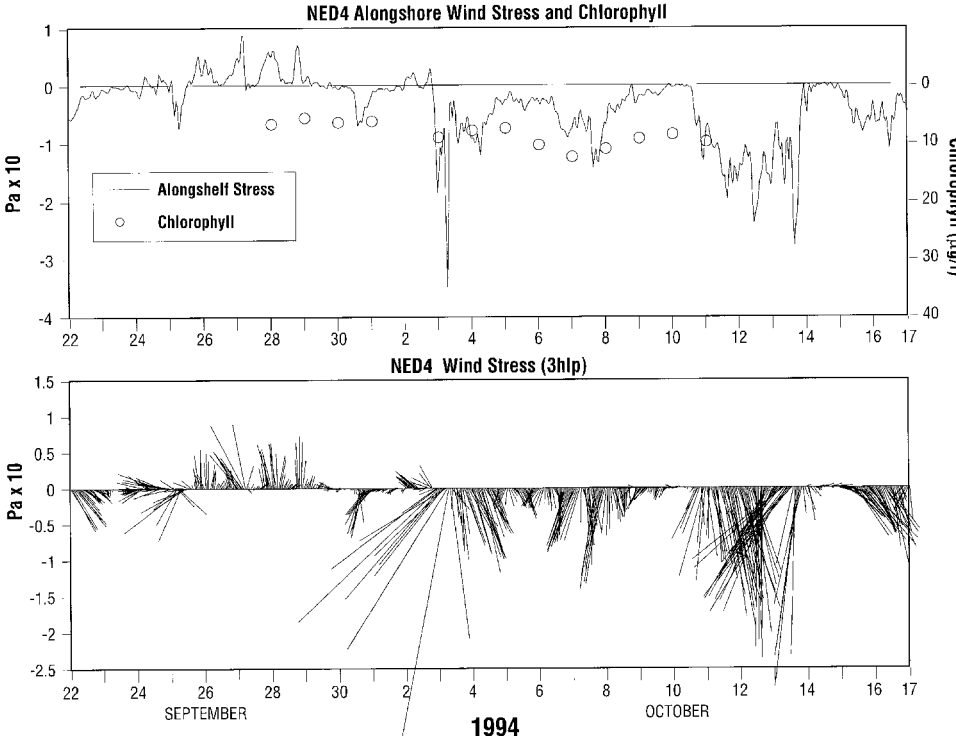

Figure 9. Temporal record of the alongshore component of 3hlp wind stress (positive component alongshore toward NE) and chl *a* (top panel) and wind vectors (bottom panel) in September 1994. Chl *a* data points represent water column mean values for each flood tide sampling period, and typically included 8–15 profiles binned at 1 m intervals.

sample period (Fig. 11b), and with alongshore wind stress, which increases with the square of speed (Figs. 12a,b). Similar patterns were not observed between chl *a* and *x*-axis (cross-shelf) components of wind.

c. Effects of tidal currents

To investigate temporal and spatial patterns in chl *a* distributions further, time series sampling was conducted at two locations on the delta in June 1994 and at three locations in September 1994. A current meter was deployed one meter above the bottom at each location and vertical profiles were conducted at ca. hourly intervals (see Methods). Sample locations had similar depth horizons and were chosen because historical and anecdotal data suggested that seawater might enter/exit the estuary not only through the main channel near site NA1 but also via channels adjacent to sites SA3 and NA3 (Fig. 1). Technical problems prevented sampling of complete tidal cycles during both experiments, but continuous sampling was achieved for 12 hours (June) and 27 hours (September).

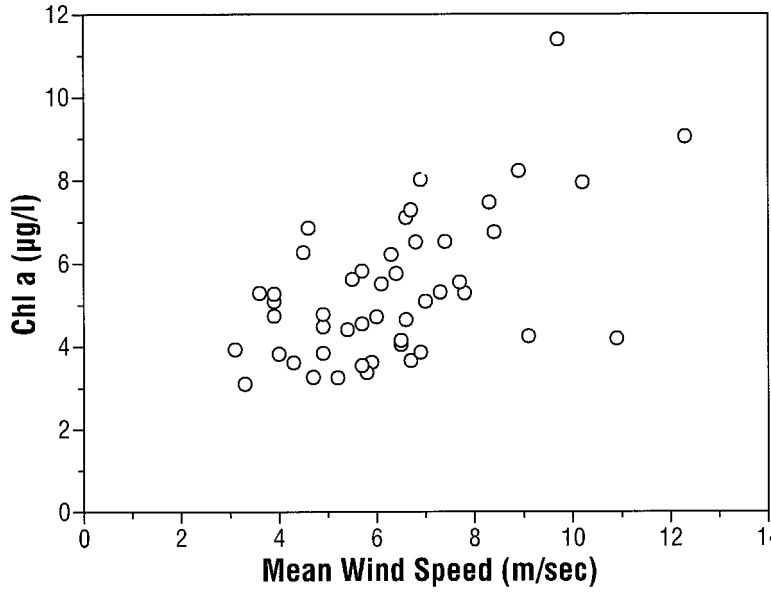

Figure 10. Relationships between chlorophyll *a* and mean wind speed (m sec^{-1}) for all data in 1993 and 1994. Each wind speed data point represents the mean value (including all wind directions) measured during the period of sampling (typically 4–6 hours) plus the preceding 6 hours (see text). Each chl *a* data point represents the water column mean value for each flood tide sample period (as in Fig. 9). Model regression: Chl a = (Mean average wind speed) (0.65) + 2.85, $r^2 = 0.32, n = 48$.

Current meter measurements indicated that current structure was complex and not synchronous at the three locations (Fig. 13). Tidal current vectors typically trace out an ellipse in coastal waters (Pietrafesa *et al.,* 1985). Despite sampling through a complete tidal cycle in September 1994, current vectors were shoreward most of the time at all locations (Fig. 14). At the two sites closest to shore (SA3, NA3), vectors were alongshore with only slight seaward motion even during full ebb tide. Current speeds varied through the tidal cycle between 0 and 30 cm/s at NA1 and SA3 and 0 and 60 cm/s at NA3 illustrating the varying strength of the currents in a relatively short distance. There was no distinct tidal cycle in either temperature or salinity on the delta. Local winds may have influenced current patterns on the shallow delta. For example, the currents measured on the delta had variations that appear related to the onshore and upwelling-favorable sea breeze which sprang up during the afternoon of the first ebb tide in September (winds were calmer during the second cycle). The current during flood tide at the middle station was northward, while ebb tide was eastward, which was approximately perpendicular to the isobaths at the middle station. Residual flow at the middle station was along the arc toward the northeast (downwind) at a speed of almost 16 cm/s. Thus, it appears that variations in wind stress during the 2 tidal cycles affected the currents.

At the site adjacent to the main channel (NA1) in June 1994, patterns in temperature and salinity indicated vertical stratification at slack water and mixing during ebb and flood tides

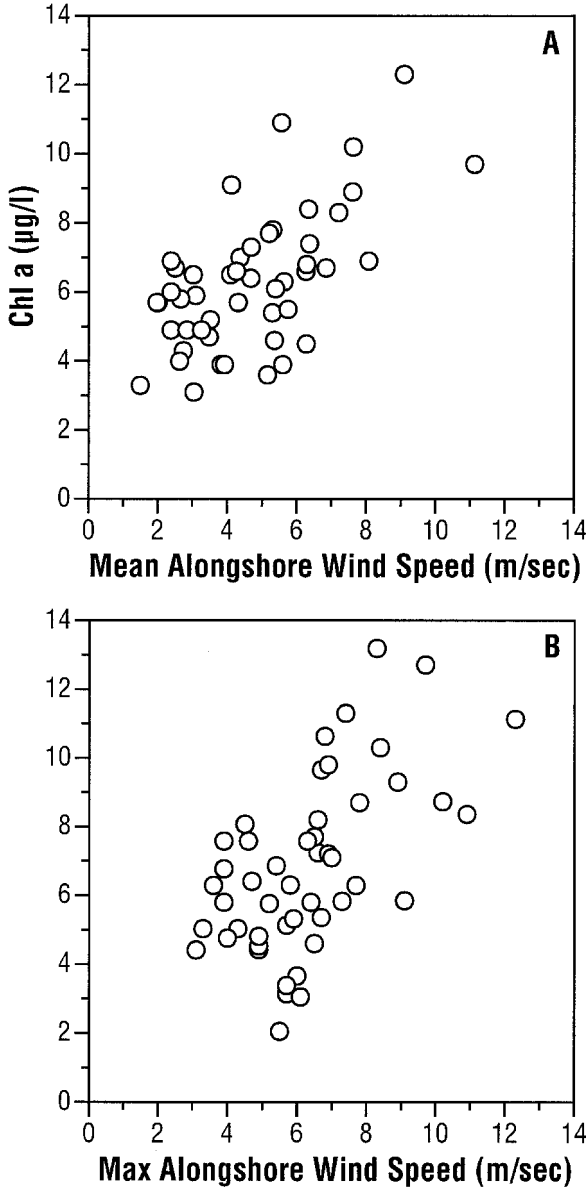

Figure 11. Relationships between chlorophyll *a* and (a) mean and (b) maximum alongshore wind speed (m sec^{-1}) for all data in 1993 and 1994. Each wind speed data point represents the mean or maximum value measured during the period of sampling (typically 4–6 hours) plus the preceding 6 hours (see text). Each chl *a* data point represents the water column mean value for each flood tide sample period (as in Fig. 9). Model regressions: (a) Chl a = (Mean alongshore wind speed) (0.60) + 3.46, $r^2 = 0.40$, $n = 48$; (b) Chl a = (Maximum alongshore wind speed) (0.50) + 2.79, $r^2 = 0.35$, $n = 48$.

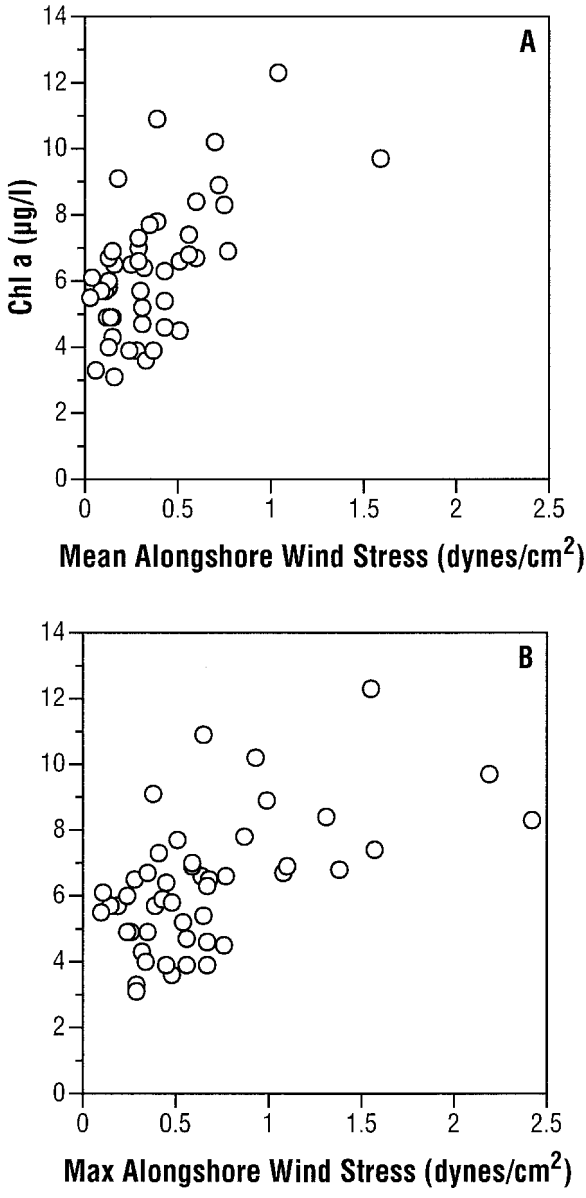

Figure 12. Relationships between chlorophyll *a* and (a) mean and (b) maximum alongshore wind stress (dynes cm^{-2}) for all data in 1993 and 1994. Each wind stress data point represents the mean or maximum value measured during the period of sampling (typically 4–6 hours) plus the preceding 6 hours (see text). Each chl *a* data point represents the water column mean value for each flood tide sample period (as in Fig. 9). Model regressions: (a) Chl a = (Mean alongshore wind stress) (4.19) + 4.83, $r^2 = 0.37$, $n = 48$; (b) Chl a = (Maximum alongshore wind stress) (2.26) + 4.82, $r^2 = 0.32$, $n = 48$.

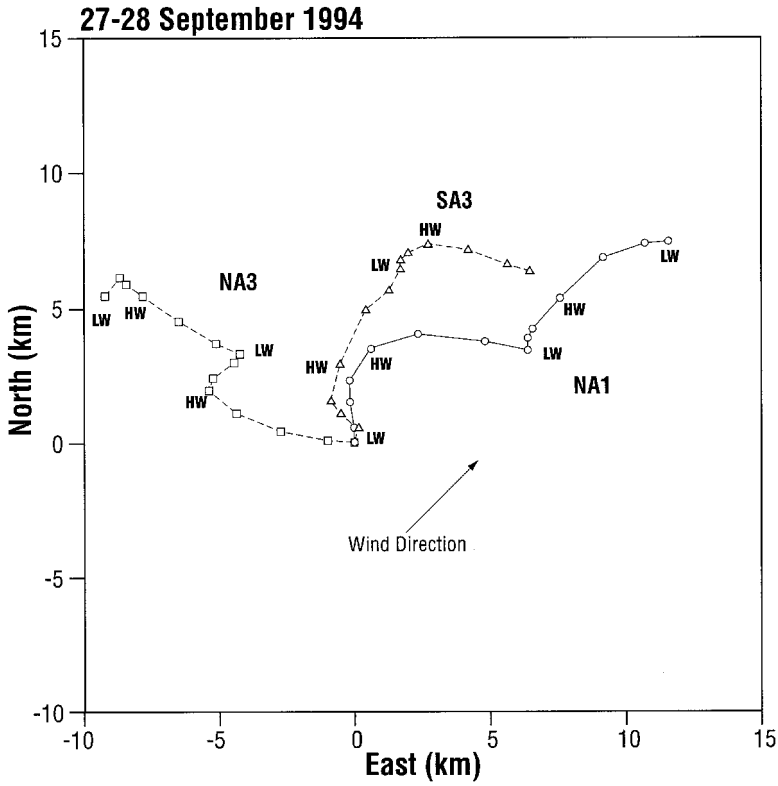

Figure 13. Progressive current vector diagrams for data collected at three sites (SA3, NA1, NA3) on the estuary delta in September 1994. Numbers represent hours since mean low water. Times of slack high water (HW) and low water (LW) are also shown.

(Fig. 15). Chl *a* exhibited similar temporal patterns with two salient characteristics: (a) pigment concentrations increased from high to low tide, and then decreased during flood tide; and (b) stratification at slack low tide coincided with near-bottom peaks in chl *a*.

Microscopy showed that the composition of the suspended phytoplankton community changed in predictable fashion during the tidal period (Fig. 16). The fraction of the total diatom community which was composed of pennate diatoms, and centric diatoms bound together in detrital material or attached to mineral grains, increased during ebb and flood tides and was lowest at slack water. These increases were substantial, such that pennates (Fig. 16a) and detrital-associated centrics (Fig. 16b) together composed ca. ¾ of all diatoms during times of maximum tidal current velocity.

Another illustration of the magnitude of tidal current mixing is comparison of the fraction of chl *a* in near-surface waters (upper 1 m) compared to that near the bottom (lower 1 m), versus current velocity (Figs. 17–18). Low ratios indicate stratification with a near-bottom chl *a* maximum, while high ratios reflect homogenization. In June, limited sampling showed a sharp decrease in stratification beginning at current speeds of

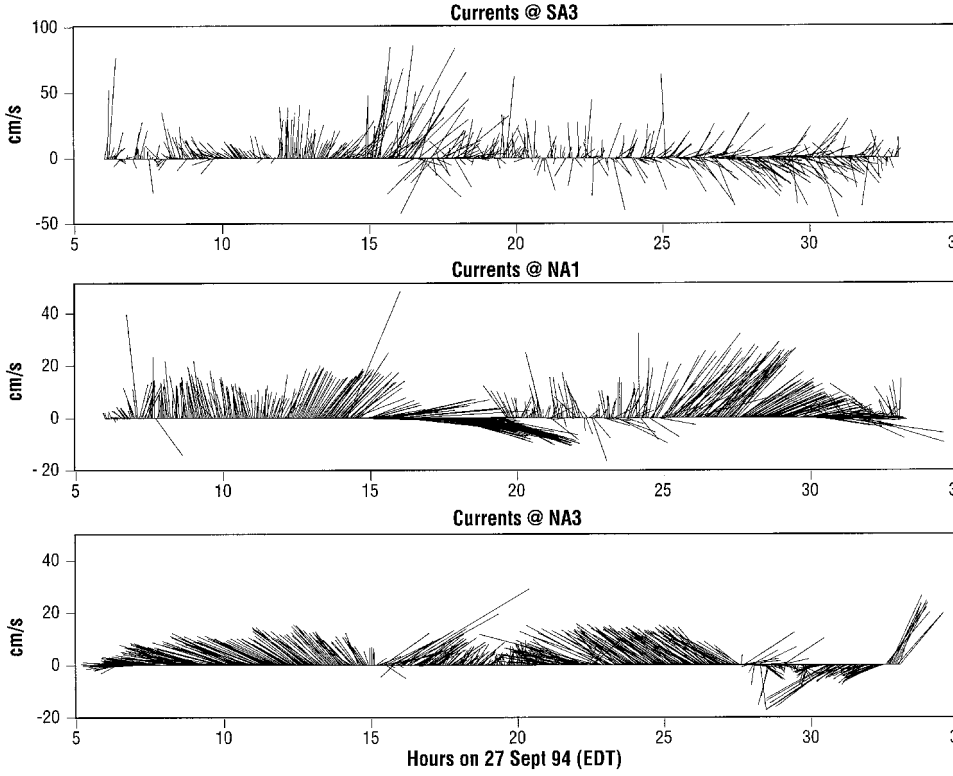

Figure 14. Current vectors for the three sites in Figure 13. Sampling interval between vectors is 3 minutes.

10 cm/sec, with homogenization nearly complete at 20 cm/sec (Fig. 17a). More complete sampling in September exhibited a similar relationship, with more scatter reflecting that measurements were taken aboard two ships at three locations (Fig. 17b). Combining both datasets suggests that pigment stratification decreases with increasing current speeds from 5 cm/sec to ca. 25 cm/sec (Fig. 17c). There were indications that the relationship between vertical stratification of chl *a* and current speed may vary somewhat between tidal phases. During ebb tide, homogenization was achieved at ca. 20 cm/sec (Fig. 18a) while 25–30 cm/sec was required during flood tides (Fig. 18b). During both tidal phases, there was a suggestion that re-stratification began at very high tidal speeds.

4. Discussion

Vertical mixing of freshwater discharge into the South Atlantic Bight produces a low density coastal frontal zone (Blanton and Atkinson, 1983; Blanton *et al.,* 1989b). River discharge and heating-induced buoyancy inhibit vertical and horizontal fluxes of momentum and particles, and determine the cross-frontal structure of the coastal zone. A

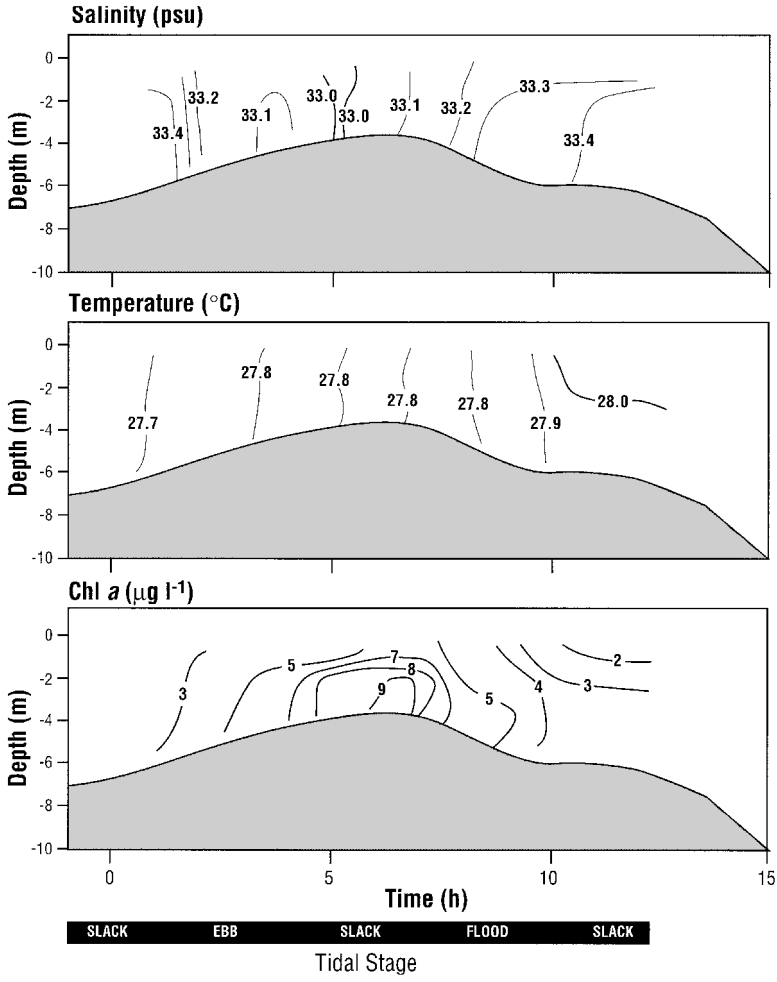

Figure 15. Time series plots of salinity, temperature, and chl *a* during sampling at station NA1 on June 17, 1994, derived from vertical profiles collected at ca. hourly intervals beginning at 0300 h.

density-driven cross-frontal circulation pattern emanates from the positive density gradient extending outward from the shoreline. Onshore flow is encouraged by a near-bottom, seaward baroclinic pressure gradient. Near the surface, the offshore directed barotrophic pressure gradient overwhelms the onshore baroclinic gradient, and offshore flow predominates.

Superimposed on this current regime are wind-generated upwelling and downwelling cycles which modify rise and fall of coastal sea level. During upwelling, the coastal front spreads seaward and enhances the vertical density gradient (Chao, 1987), reinforcing the density-driven current regime. During downwelling, the frontal zone is typically well defined and the vertical density gradient is minimized. When alongshore winds reverse for

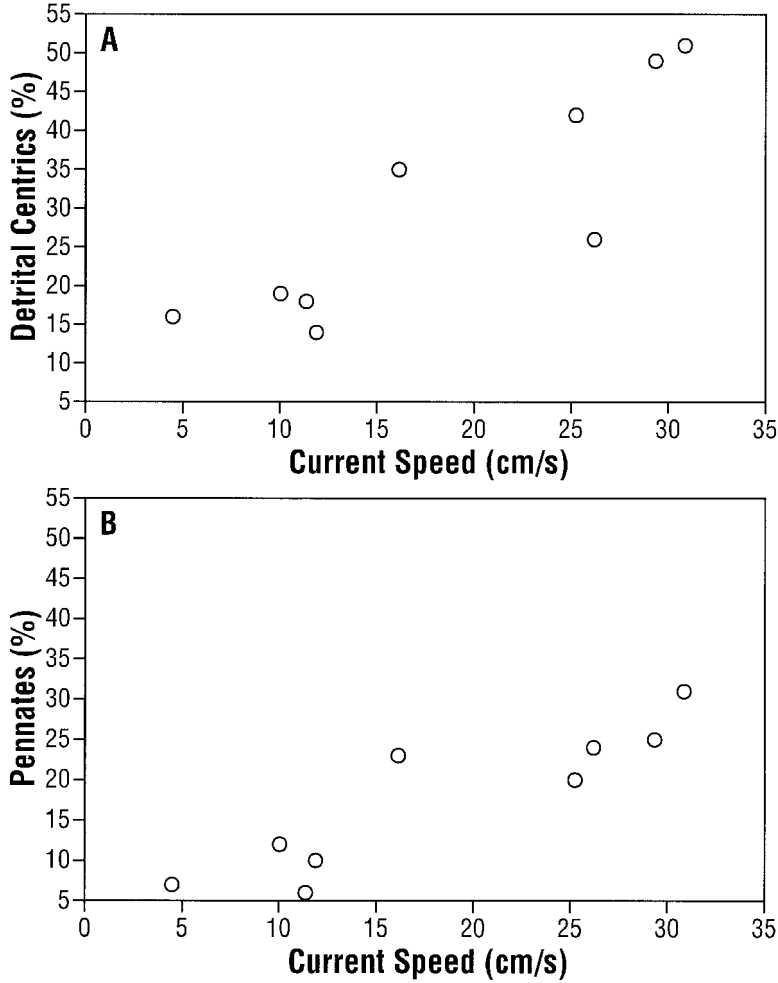

Figure 16. Relationships between the fraction of total diatom abundance represented by (a) centric diatoms attached to detrital material and sand grains, and (b) pennate diatoms, versus tidal current velocity. Data were from station NA1 in June 1994.

as little as 6 h, the current regimes adjust rapidly and may be accompanied by strong cross-shelf circulation (Blanton *et al.,* 1989b). Such reversals, which typically occur at intervals of 3–7 days, shifted the location of the 34 PSU isohaline off the North Edisto estuary by 7–10 km; however, chl *a* isopleths were not similarly affected. Likewise, the vertical distribution of chl *a* in inner shelf waters was nearly homogenous, and under upwelling-favorable conditions chl *a* did not exhibit the strong vertical gradients typical of salinity. There may be several, nonexclusive explanations for this lack of vertical stratification in chl *a:* relative reductions of fast-settling large diatoms, relative increases of motile small phytoplankton, and balances between cell growth in the upper euphotic zone

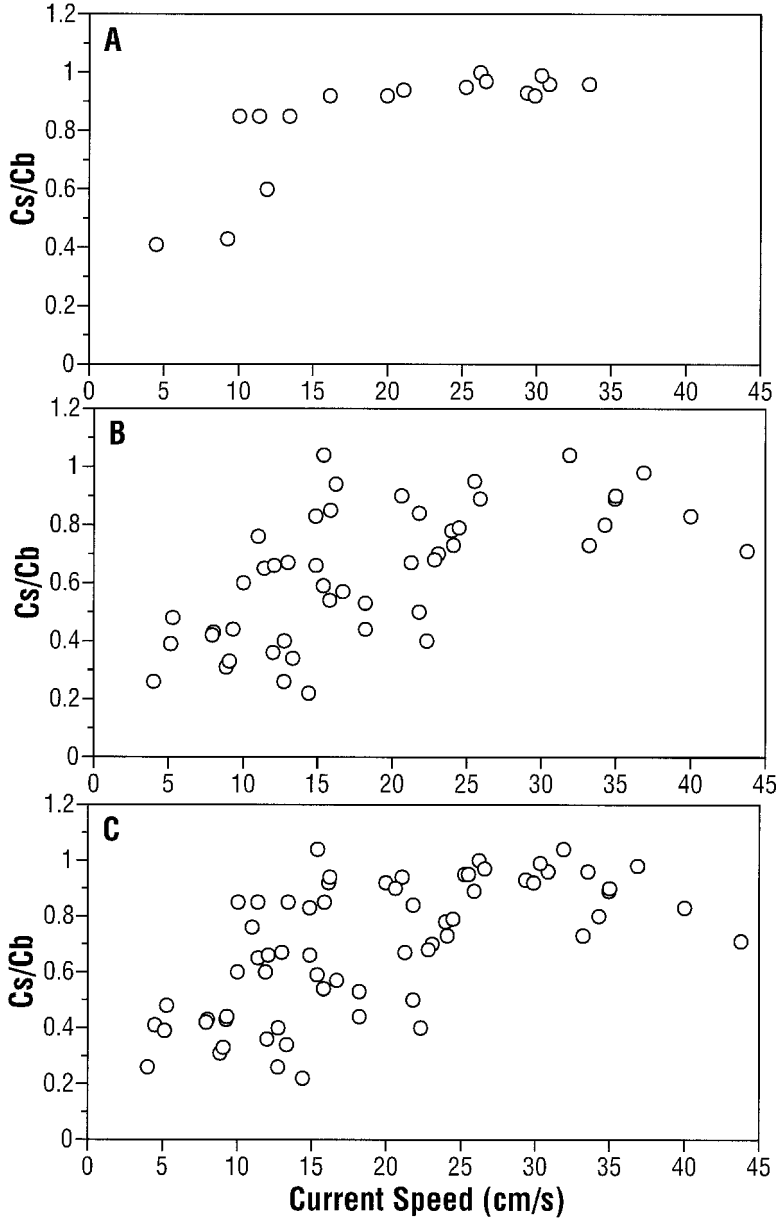

Figure 17. Relationships between the fraction of chl *a* in near-surface waters (0–1 m) relative to that in near-bottom waters (within 1 m of bottom), versus tidal current velocity. Data were from stations (a) NA3 and NA1 in June 1994; (b) NA3, NA1, and SA3 in September 1994; and (c) all stations in June and September combined.

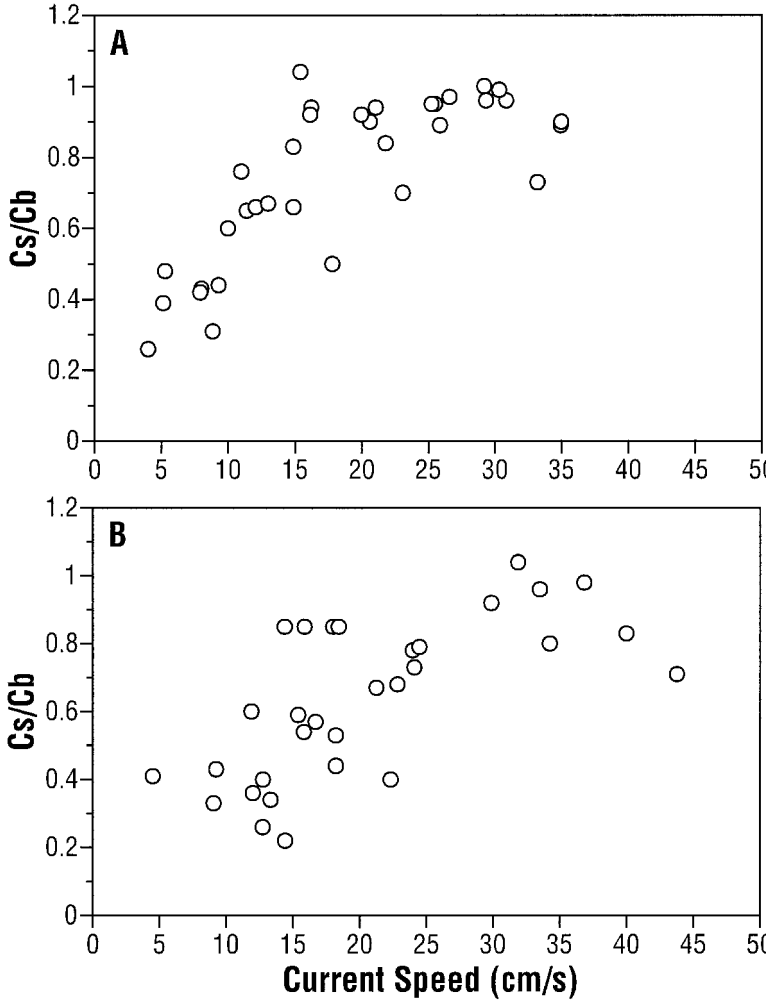

Figure 18. Relationships between the fraction of chl *a* in near-surface waters (0–1 m) relative to that in near-bottom waters (within 1 m of bottom), versus tidal current velocity. Data were from (a) all samples collected during ebb tides, and (b) all samples collected during flood tides, in June and September 1994.

and cell sinking to depth. Chl *a* decreased with increasing distance offshore and increasing salinity, indicating that the North Edisto estuary and/or ebb tide delta was a significant source of phytoplankton for inner shelf waters, as observed in adjacent Georgia coastal waters (Verity *et al.,* 1993; Yoder *et al.,* 1993).

In the estuary throat, chl *a* concentrations were positively correlated with wind speed and wind stress. Since these relationships held during May-June and August-October over a two year period, a strong argument can be made that winds influence phytoplankton

biomass in these waters, at least during spring, summer, and autumn. Stronger winds were associated with greater chl *a* increases, but even moderate winds apparently induced elevated chl *a* concentrations. The short response time between changes in wind strength and in phytoplankton biomass, generally 6–12 hours, most of which coincided with periods of darkness, implies a direct effect of wind on chl *a* rather than stimulation of growth rate as observed elsewhere (Kiorboe and Nielsen, 1990). Interestingly, the data also suggest that processes responsible for accumulation and loss of chl *a* were approximately in balance for comparatively long periods, because (a) the chl *a*-salinity relationship with distance offshore was maintained for at least two week intervals; and (b) the chl *a*-wind relationships, which were evident during four two-week periods, would have disintegrated if other increment-loss processes were varying substantially over time.

The highest chl *a* concentrations in the estuary throat coincided with strong downwelling wind events (local winds from NE). The pattern of chl *a* increasing with salinity during these events (Fig. 6b) reflects that sampling occurred during flooding tide: salinity increased as shelf water migrated into the estuary, but this saline water, which contained less chl *a* when residing on the shelf (Figs. 4), somehow incorporated more chl *a* under strong downwelling-favorable winds. High concentrations of chl *a* occurred on the estuary delta (Figs. 2–3) and the tidal excursion of 6–8 km was sufficient to transport these waters and resident particles into the estuary throat. The near-bottom maxima of chl *a* both on the delta and in the estuary throat imply that a major source of this elevated chl *a* was resuspension of settled and/or epibenthic algal cells, a conclusion supported by the time series current meter and phytoplankton composition analyses. We argue that the positive correlation between winds and chl *a* reflects resuspension of the near-bottom chl *a* maxima, caused by the alongshelf wind stress increasing the turbulence at the bottom in the form of waves and downwind currents which move water primarily along isobaths. The vector plots of wind stress (Fig. 9) indicate that, except for a few isolated events, the cross-shelf wind stress component is relatively weak compared to the alongshelf component. The coastal barrier makes motion across isobaths increasingly difficult in the shallow water near the coast except at the mouths of estuaries and inlets. Compared to along-isobath motion, more work must be expended to move water across isobaths, a fact that is supported by relatively small cross-isobath current components (Blanton *et al.,* 1989b). Moreover, any net cross-isobath motion due to wind-generated waves is a relatively small second-order effect. Since only the wind component parallel to the shoreline is able to move water efficiently, it is not surprising that chl *a* concentrations bore little relationship to cross-shelf wind stress. This notion is further supported by our observations that the strength of the alongshelf wind component has a greater impact on chl *a* concentrations than does its direction. Independent of direction, wind generated alongshelf flow as it encounters the arcuate delta converges along the steep flank where velocities are presumably increased. Short-term moorings along the arcuate delta further indicated that tidal currents achieved their maximum strength at the steep edge of the delta (Wenner *et al.,* 1998).

Mixing is provided by tidal currents due to frictional effects which reduce current velocity with depth in the water column. Current velocities in 5–7 m water columns were sufficient to resuspend epibenthic pennate diatoms, as confirmed by microscopic investigation (Fig. 16b). These cells may be photosynthetic in the water column and on the bottom in shallow waters, and some are likely obligately or facultatively heterotrophic, especially considering the high organic content of nearshore SAB sediments (Admiraal and Peletier, 1979). During flood tides, when "new" water from offshore which contains less chl *a* is added to the water column of the delta and estuary, the integrated chl *a* should decrease. This was not observed, indicating that "new" chl *a* was added separately but concurrently with dilute offshore water: this new chl *a* was partially in the form of resuspended pennate diatoms.

The other major contributor to resuspended microalgal biomass was centric diatoms enmeshed in detrital and inorganic particles (Fig. 16a). These diatoms included several species of *Thalassiosira,* at least one of which, resembling *T. eccentrica,* is known to directly bind to quartz and feldspar grains in the silt size range in these waters (Ernissee and Abbott, 1975). The binding mechanism, thought to be a siliceous web, resists strong chemical and high heat treatments (Ernissee and Abbott, 1975), and thus the affiliation of the diatoms with the sedimentary material should be maintained even in the presence of strong mixing. The explanation for this binding to heavy particles by photosynthetic organisms living in a turbid, light-limited environment is perhaps not intuitive. However, other diatoms are known to deliberately adjust their buoyancy as a mechanism to acquire nutrients from depth when they are limiting in the upper euphotic zone (Villareal and Carpenter, 1994; Richardson and Cullen, 1995). In shallow turbulent environments, where permanent loss from the euphotic zone is minimized, becoming artificially heavy might facilitate regular contact or close proximity to nutrient-rich sediments, followed by regular exposure to irradiance to utilize those recently acquired nutrient stores. Primary productivity in these waters is quite high, despite low ambient nutrient concentrations (Verity *et al.,* 1993).

The entrainment of epibenthic and settled microalgae into shallow water columns is well documented (Shaffer and Sullivan, 1988; MacIntyre and Cullen, 1995; citations therein). In the nearshore SAB, tidal currents and wave resuspension are the major factors responsible for variations in suspended particle concentrations (Oertel and Dunstan, 1981). Off Wassaw Sound, Georgia, ca. 70 km south of the North Edisto estuary, pennate diatoms contributed 8–65% of total suspended diatom abundance (Oertel and Dunstan, 1981), similar to observations in the North Edisto. Elsewhere, resuspended microalgae contribute significantly to chl *a* and, apparently, to primary productivity (Roman and Tenore, 1978; Baillie and Welsh, 1980; Shaffer and Sullivan, 1988), although the increase in water column productivity due to resuspended cells will be offset by increased turbidity associated with resuspended sediments (MacIntyre and Cullen, 1995). Additional sources of resuspended chl *a* in the SAB may be from taxa growing on salt marsh and tidal creek surfaces (Pomeroy, 1959; Gallagher, 1975), especially during spring tides when lagoonal

tidal prisms are two-three times greater than mean and neap prisms, respectively (Oertel and Dunstan, 1981).

It is a well-known phenomenon to even casual observers of SAB estuaries and coastal waters that water clarity is maximal at slack water and minimal during ebb and flood. In the North Edisto, chlorophyll-containing particles began to mix upward at tidal current velocities of only 10 cm/sec, and complete mixing of 5–7 m water columns was achieved at 30 cm/sec. These velocities are at the low end of ranges observed in southeastern coastal waters, implying that resuspension occurs broadly and regularly. These data support the conclusions from tank experiments where resuspension of benthic diatoms, including those attached to sand grains, began at velocities of 10 cm/sec (de Jonge and van den Bergs, 1987). Other tank tests showed that current velocities of 20–29 cm/sec, while resuspending epibenthic cells, also sequentially buried and unburied chl *a* through the mechanism of ripple formation (Jenness and Duineveld, 1985). To the extent that such burial and subsequent resuspension occurs in SAB coastal waters, it might provide the mechanism of attachment for those bound to detrital and sedimentary particles. This resuspension may also partially account for observed patchiness of chl *a* in nearby estuarine and inner shelf waters (Dustan and Pinckney, 1989).

Resuspension is not limited to chlorophyll-containing cells but also smaller (Wainright, 1990) and larger organisms (Palmer and Gust, 1985). Moored acoustic data collected during the present study (Barans *et al.,* 1997) indicate that particles up to ca. 100 μm in size are resuspended in the North Edisto estuary during ebb and flood tides. Resuspension appeared proportional to velocity as observed for chl *a* on the delta, because resuspension was greater during spring than neap tides, and greater during the faster ebb than the slower flood tides. Resuspension of sediment particles elsewhere occurred after tidal current velocities exceeded a critical threshold of 20 cm/sec (Grabemann and Krause, 1989), similar to that observed here for chlorophyll-containing particles. Since tidal current velocities in the North Edisto, and by implication other SAB estuaries, well surpass this threshold, it can be assumed that resuspension occurs during most, if not all, tidal cycles.

The effects of winds on phytoplankton distributions have been studied for decades, often focussing on stimulation of the productivity of suspended cells (Iverson *et al.,* 1974; Kiorboe and Nielsen, 1990). Resuspension of settled and benthic algae by winds has also been previously reported. However, these events occurred in comparatively shallow waters, e.g., estuaries (2 m: Gabrielson and Lukatelich, 1985), tidal flats (2–3 m: de Jonge and van Beusekom, 1995), and shallow embayments (2–6 m: Demers *et al.,* 1987). The present data show wind-related enhancements of chl *a* in coastal waters 10–20 m deep. Also unusual is that the relationship between wind speed and chl *a* in the North Edisto system was linear over the entire range of mean wind speed observed (range = 0–11 m/sec). The above prior studies all reported thresholds below which wind effects were not apparent, typically 3–5 m/sec, despite the fact that those waters were shallower than the North Edisto environment. This may reflect the fact that substantial proportions of the resuspended chl *a* in the North Edisto apparently came from settled phytoplankton, which

may resuspend more readily than benthic diatoms. The latter, which were the source of the enhanced chl *a* in the other studies, attach to clay and mineral grains (de Jonge, 1985) and function to stabilize sediments (Delgado *et al.,* 1991). The present linear relationships may not necessarily hold at very high wind speeds because the source material is not limitless (de Jonge and van Beusekom, 1995). Higher concentrations of phaeopigments were also found during wind events in the North Edisto (data not shown), as reported for shallow embayments in the lower St. Lawrence estuary (Demers *et al.,* 1987), implying resuspension of degraded chl *a.*

Because the alongshore component dominates the overall mean wind speed vector, the two are related. For the 70 days of sampling in 1993 and 1994, the following linear regression describes the relationship between the *y*-component (alongshore) speed and the combined mean speed (all directions included): *y*-wind speed (m/sec) = (combined wind speed) (1.12) − 1.41, $r^2 = 0.89$. Using this model regression and that observed between chl *a* and combined wind speed (Fig. 10), the annual impact of wind mixing on chl *a* in the water column can be estimated. Archived meterological data for the Folly Beach meterological station adjacent to the study site were obtained from the U.S. National Oceanographic and Atmospheric Administration (NOAA) National Buoy Data Center (NBDC). Collected at hourly intervals, mean combined wind speeds (all directions included) were calculated for study years 1993 (4.7 m/sec) and 1994 (5.1 m/sec). Inserting the two year mean wind into the regression model of Figure 14 predicts an annual chl *a* concentration of 2.8 μg/l in the absence of wind, and 6.0 μg/l in the presence of a mean wind field of 4.9 m/sec. Thus, local winds are predicted to double the average concentration of phytoplankton biomass in North Edisto waters on an annual basis. Since climatology, wind fields, inlet geology, and phytoplankton biomass are similar throughout inner shelf waters of the South Atlantic Bight (Oertel and Dunstan, 1981; Atkinson *et al.,* 1985; Menzel, 1993), the effects of winds on suspended phytoplankton biomass may be widespread; exceptions would include natural or anthropogenically-induced (e.g. dredged channels) deeper waters.

The trophic implications of a doubling or similar substantial increase in suspended phytoplankton biomass may be significant. Chl *a* concentrations of 3–6 $\mu g \cdot l^{-1}$ typically include the linear response portion of filtering rate curves for herbivorous zooplankton (Paffenhöfer and Van Sant, 1985) and fish (Friedland *et al.,* 1984) in these waters. Thus, resuspended phytoplankton may provide enhanced food availability for higher trophic levels (e.g. de Jonge and van Beusekom, 1992), contributing to the substantial fin and shellfish productivity in coastal and estuarine waters of the South Atlantic Bight. Moreover, wind and tidal resuspension of phytoplankton may function as a "nutritional hypodermic," injecting flood tides containing immigrating organisms, e.g. postlarval white shrimp and blue crabs (Wenner *et al.,* 1998), with elevated food concentrations.

The high productivity of these waters dictates that standing stocks of plankton, detritus, and nutrients must be cycling rapidly, and changing on hourly and diel timescales especially (Hanson *et al.,* 1988, 1990; Pomeroy *et al.,* 1993; Verity *et al.,* 1993). Yet consumption processes often keep pace with production during periods when physical

processes permit an approach towards steady state. The present data illustrate that, in estuary mouths and adjacent coastal waters, local winds and tidal currents distribute phytoplankton in space and time. When physical processes change scale or state, e.g. reversals from upwelling- to downwelling-favorable regimes at 3–7 day intervals or during more stochastic strong downwelling events, biological populations chart a new temporary course toward a new steady state. Thus, while biological processes in these shallow productive waters are closely linked and highly interdependent (Verity *et al.,* 1993), physical control of biological populations is still a fundamental ecosystem characteristic.

Acknowledgments. The authors thank S. C. Williams, C. Petrie, and M. Ward for sample collection and analysis. The captains and crews of the R/V *Blue Fin* and *Anita* provided competent and friendly service all night long, often under challenging weather conditions, e.g. southeast U.S. summer thunderstorms. This research was only possible through the close cooperation of the Georgia and South Carolina Sea Grant programs, under the capable stewardship of Drs. M. Rawson and M. Davidson/R. DeVoe, respectively, reflecting Sea Grant awards NA26RG-0-37301 to JOB and PGV, and 93277 to ELW and CAB. D. Peterson prepared the manuscript and A. Boyette drafted the figures.

REFERENCES

Admiraal, W. and H. Peletier. 1979. Influence of organic compounds and light limitation on the growth rate of estuarine benthic diatoms. Br. Phycol. J., *14,* 197–206.

Atkinson, L. P., D. W. Menzel and K. A. Bush, eds. 1985. Oceanography of the Southeastern U.S. Continental Shelf. Coastal and Estuarine Sciences, *2,* AGU, Washington, DC, 156 pp.

Baillie, P. W. and B. L. Welsh. 1980. The effect of tidal resuspension on the distribution of intertidal epipelic algae in an estuary. Estuar. Coast. Mar. Sci., *10,* 165–180.

Barans, C. A., B. W. Stender, D. Van Holliday and C. F. Greenlaw. 1997. Variation in the vertical distribution of zooplankton and fine particles in an estuarine inlet of South Carolina. Estuaries, *20,* 467–482.

Blanton, J. O. 1981. Ocean currents along a nearshore frontal zone on the continental shelf of the southeastern United States. J. Phys. Oceanogr., *11,* 1627–1637.

—— 1991. Circulation processes along oceanic margins in relation to material fluxes, *in* Ocean Margin Processes in Global Change, R. F. C. Mantoura, J.-M. Martin, and R. Wollast, eds., John Wiley & Sons, NY, 146–163.

Blanton, J., J. Amft, D. Lee and A. Riordan. 1989a. Wind stress and heat fluxes observed during winter and spring 1986. J. Geophys. Res., *94,* 10,686–10,698.

Blanton, J. O., J. Amft and P. G. Verity. 1994a. The May 1993 North Edisto Ingress Experiment (NED1). Georgia Marine Science Center, Technical Report Series 94-1, Skidaway Island, GA, USA.

—— 1997. The August 1993 North Edisto Ingress Experiment (NED2). Georgia Marine Science Center, Technical Report Series 97-1, Skidaway Island, GA, USA.

Blanton, J. O. and L. P. Atkinson. 1983. Transport and fate of river discharge on the continental shelf of the southeastern United States. J. Geophys. Res., *88,* 4730–4738.

Blanton, J. O., L.-Y. Oey, J. Amft and T. N. Lee. 1989b. Advection of momentum and buoyancy in a coastal frontal zone. J. Phys. Oceanogr., *19,* 98–115.

Blanton, J. O., F. Werner, C. Kim, L. Atkinson, T. Lee and D. Savidge. 1994b. Transport and fate of low-density water in a coastal frontal zone. Cont. Shelf Res., *14,* 401–427.

Chao, S.-Y. 1987. Wind-driven motion near inner shelf fronts. J. Geophys. Res., *92,* 3849–3860.

Cloern, J. E. 1991. Tidal stirring and phytoplankton bloom dynamics in an estuary. J. Mar. Res., *49,* 203–221.

de Jonge, V. N. 1985. The occurrence of 'epipsammic' diatom populations: a result of interaction between physical sorting of sediment and certain properties of diatom species. Estuar. Coast. Shelf Sci., *21,* 607–622.

de Jonge, V. N. and J. van den Bergs. 1987. Experiments on the resuspension of estuarine sediments containing benthic diatoms. Estuar. Coast. Shelf Sci., *24,* 725–740.

de Jonge, V. N. and J. E. E. Van Beusekom. 1992. Contribution of resuspended microphytobenthos to total phytoplankton in the Ems estuary and its possible role for grazers. Neth. J. Sea Res., *30,* 91–105.

—— 1995. Wind- and tide-induced resuspension of sediment and microphytobenthos from tidal flats in the Ems estuary. Limnol. Oceanogr., *40,* 766–778.

Delgado, M., V. N. de Jonge and H. Peletier. 1991. Experiments on resuspension of natural microphytobenthos populations. Mar. Biol., *108,* 321–328.

Demers, S., J.-C. Therriault, E. Bourget and A. Bah. 1987. Resuspension in the shallow sublittoral zone of a macrotidal estuarine environment: wind influence. Limnol. Oceanogr., *32,* 327–339.

Dustan, P. and J. L. Pinckney, Jr. 1989. Tidally induced estuarine phytoplankton patchiness. Limnol. Oceanogr., *34,* 410–419.

Ernissee, J. J. and W. H. Abbott. 1975. Binding of mineral grains by a species of *Thalassiosira.* Nova Hedwigia Beih., *53,* 241–248.

Friedland, K. D., L. W. Haas, and J. V. Merriner. 1984. Filtering rates of the juvenile Atlantic menhaden *Brevoortia tyrannus* (Pisces: Clupeidae), with consideration of the effects of detritus and swimming speed. Mar. Biol., *84,* 109–117.

Gabrielson, J. O. and R. J. Lukatelich. 1985. Wind-related resuspension of sediments in the Peel-Harvey estuarine system. Estuar. Coast. Shelf Sci., *20,* 135–145.

Gallagher, J. L. 1975. The significance of the surface film in salt marsh plankton metabolism. Limnol. Oceanogr., *29,* 120–123.

Garvine, R. W. 1991. Subtidal frequency estuary-shelf interaction: observations near Delaware Bay. J. Geophys. Res., *96,* 7049–7064.

Grabemann, I. and G. Krause. 1989. Transport process of suspended matter derived from time series in a tidal estuary. J. Geophys. Res., *94,* 14,373–14,379.

Hanson, R. B., L. R. Pomeroy, J. O. Blanton, B. A. Biddanda, S. Wainwright, S. S. Bishop, J. A. Yoder and L. P. Atkinson. 1988. Climatological and hydrographic influences on nearshore foodwebs off the southeastern United States: bacterioplankton dynamics. Cont. Shelf Res., *8,* 1321–1344.

Hanson, R. B., C. Y. Robertson, J. A. Yoder, P. G. Verity and S. S. Bishop. 1990. Nitrogen recycling in coastal waters of southern U.S. during summer 1986. J. Mar. Res., *48,* 641–660.

Iverson, R. L., H. C. Curl, Jr., H. B. O'Conners, Jr., D. Kirk and K. Zakar. 1974. Summer phytoplankton blooms in Auke Bay, Alaska, driven by wind mixing of the water column. Limnol. Oceanogr., *19,* 271–278.

Jenness, M. I. and G. C. A. Duineveld. 1985. Effects of tidal currents on chlorophyll *a* content of sandy sediments in the southern North Sea. Mar. Ecol. Prog. Ser., *21,* 283–287.

Kiorboe, T. and T. G. Nielsen. 1990. Effects of wind stress on vertical water column structure, phytoplankton growth, and productivity of planktonic copepods, *in* Trophic Relationships in the Marine Environment, Proc. 24th Europ. Mar. Biol. Symp., M. Barnes and R. N. Gibson, eds., Aberdeen University Press, 28–40.

Kjerfve, B. J. and J. A. Proehl. 1979. Velocity variability in a cross-section of a well-mixed estuary. J. Mar. Res., *37,* 407–418.

MacIntyre, H. L. and J. J. Cullen. 1995. Fine-scale vertical resolution of chlorophyll and photosynthetic parameters in shallow-water benthos. Mar. Ecol. Prog. Ser., *122,* 227–237.

Matthews, T. D. and H. H. Shealy, Jr. 1978. Hydrography of South Carolina estuaries with emphasis on the North and South Edisto and Cooper Rivers. S. C. Mar. Res. Center Technical Report No. 30, 148 pp.

Menzel, D. W., ed. 1993. Ocean Processes: U.S. Southeast Continental Shelf: a summary of research conducted in the South Atlantic Bight under the auspices of the U.S. Department of Energy from 1977 to 1991. U.S. Department of Energy, Office of Science and Technical Information, DOE/OSTI—11674, 112 pp.

Monbet, Y. 1992. Control of phytoplankton biomass in estuaries: a comparative analysis of microtidal and macrotidal estuaries. Estuaries, *15,* 563–571.

Nixon, S. W. 1988. Physical energy inputs and the comparative ecology of lake and marine ecosystems. Limnol. Oceanogr., *33,* 1005–1025.

Nummedal, D., G. Oertel, D. Hubbard and A. Hine. 1977. Tidal inlet variability—Cape Hatteras to Cape Canaveral, *in* Coastal sediments 1977: 5th Symposium of the Waterway, Port, and Coastal and Ocean Division, ASCE, 543–562.

Oertel, G. F. and W. M. Dunstan. 1981. Suspended sediment distribution and certain aspects of phytoplankton production off Georgia. Mar. Geol., *40,* 171–197.

Paffenhöfer, G.-A. and K. B. Van Sant. 1985. The feeding response of a marine planktonic copepod to quantity and quality of particles. Mar. Ecol. Prog. Ser., *27,* 55–65.

Palmer, M. A. and G. Gust. 1985. Dispersal of meiofauna in a turbulent tidal creek. J. Mar. Res., *43,* 179–210.

Pietrafesa, L. J., J. O. Blanton, J. D. Wang, V. Kourafalou, T. N. Lee and K. A. Bush. 1985. The tidal regime in the South Atlantic Bight, *in* Oceanography of the Southeastern U.S. Continental Shelf, L. P. Atkinson, D. W. Menzel and K. A. Bush, eds., Coastal and Estuarine Sciences, *2,* AGU, Washington, DC, 63–76.

Pomeroy, L. R. 1959. Algal productivity in salt marshes of Georgia. Limnol. Oceanogr., *4,* 386–398.

Pomeroy, L. R., J. O. Blanton, G.-A. Paffenhöfer, K. L. Von Damm, P. G. Verity, H. L. Windom and T. N. Lee. 1993. Inner shelf processes, *in* Ocean Processes, U.S. Southeast Continental Shelf (D. W. Menzel, ed.), U.S. DOE Document DOE/OSTI-11674, 9–43.

Redfield, A. C. 1958. The influence of the continental shelf on the tides of the Atlantic coast of the United States. J. Mar. Res., *17,* 432–448.

Richardson, T. L. and J. J. Cullen. 1995. Changes in buoyancy and chemical composition during growth of a coastal marine diatom: ecological and biogeochemical consequences. Mar. Ecol. Prog. Ser., *128,* 77–90.

Roman, M. R. and K. R. Tenore. 1978. Tidal resuspension in Buzzards Bay, Massachusetts. Estuar. Coast. Mar. Sci., *6,* 37–46.

Shaffer, G. P. and M. J. Sullivan. 1988. Water column productivity attributable to displaced benthic diatoms in well-mixed shallow estuaries. J. Phycol., *24,* 132–140.

Therriault, J.-C., D. J. Lawrence and T. Platt. 1978. Spatial variability of phytoplankton turnover in relation to physical processes in a coastal environment. Limnol. Oceanogr., *23,* 900–911.

Thomas, J. P. 1966. Influence of the Altamaha River on primary production beyond the mouth of the river. M.S. thesis, Univ. of Georgia, Athens, GA, 88 pp.

Verity, P. G. and M. E. Sieracki. 1993. Use of color image analysis and epifluorescence microscopy to measure plankton biomass, *in* Handbook of Methods in Aquatic Microbial Ecology, P. F. Kemp, B. F. Sherr, E. B. Sherr and J. J. Cole, eds., Lewis Publ., London 327–338.

Verity, P. G., J. A. Yoder, S. S. Bishop, J. R. Nelson, D. B. Craven, J. O. Blanton, C. Y. Robertson and C. R. Tronzo. 1993. Composition, productivity, and nutrient chemistry of a coastal ocean planktonic food web. Cont. Shelf Res., *13,* 741–776.

Villareal, T. A. and E. J. Carpenter. 1994. Chemical composition and photosynthetic characteristics of *Ethmodiscus rex* (Bacillariophyceae): evidence for vertical migration. J. Phycol., *30,* 1–8.

Wainright, S. C. 1990. Sediment-to-water fluxes of particulate material and microbes by resuspension and their contribution to the planktonic food web. Mar. Ecol. Prog. Ser., *62,* 271–281.

Wenner, E., D. Knott, J. Blanton, C. Barans and J. Amft. 1998. Effects of oceanographic conditions on recruitment of postlarval white shrimp, *Penaeus setiferus,* to a South Carolina (USA) estuary. Mar. Ecol. Prog. Ser., (submitted).

Yin, K., P. J. Harrison, R. H. Goldblatt and R. J. Beamish. 1996. Spring bloom in the central Strait of Georgia: interactions of river discharge, winds, and grazing. Mar. Ecol. Prog. Ser., *138,* 255–263.

Yoder, J. A. 1985. Environmental control of phytoplankton production on the southeastern U.S. continental shelf, *in* Oceanography of the Southeastern U.S. Continental Shelf, L. P. Atkinson, D. W. Menzel and K. A. Bush, eds., Coastal and Estuarine Sciences, *2,* AGU, Washington, DC, 93–103.

Yoder, J. A. and S. S. Bishop. 1985. Effect of mixing-induced irradiance fluctuations on photosynthesis of natural assemblages of coastal phytoplankton. Mar. Biol., *90,* 87–93.

Yoder, J. A., P. G. Verity, S. S. Bishop and F. E. Hoge. 1993. Phytoplankton chl *a,* primary production, and nutrient distributions across a coastal frontal zone off Georgia, USA. Cont. Shelf Res., *13,* 131–141.

Received: *8 July, 1997;* revised: *24 March, 1998.*